Glass-bearing inclusions in olivine of the Chassigny achondrite:
Heterogeneous trapping at sub-igneous temperatures

M. E. VARELA[1,2*], G. KURAT[3], M. BONNIN-MOSBAH[2], R. CLOCCHIATTI[2] AND D. MASSARE[2]

[1]CONICET-UNS Departamento de Geologia, San Juan 670, (8000) Bahia Blanca, Argentina
[2]Laboratoire Pierre Süe, CEA, CNRS, CEN Saclay, F- 91191 France
[3]Naturhistorisches Museum, Postfach 417, A-1014 Vienna, Austria
*Correspondence author's e-mail address: evarela@criba.edu.ar

Abstract–Three types of glass-bearing inclusions are present in olivine and chromite of the Chassigny achondrite: pure glass, monocrystal (glass plus a single mineral grain), and multiphase (glass plus a variety of minerals) inclusions. The occurrence, texture, and mineralogy of these inclusions and the chemical composition of the glass suggest an origin by heterogeneous trapping of these phases. The glass is rich in SiO_2, Al_2O_3, Na_2O, K_2O; and poor in MgO, FeO, and CaO; and contains appreciable amounts of Cl. The compositional variability of the glass is independent of the mineral content of the inclusions. Heating experiments with final temperatures of 900, 1000, and 1200 °C were performed with Chassigny inclusions for the first time. The glass of the heated inclusions has a chemical composition similar to that of unheated inclusions. This situation suggests that the glass cannot be a residual melt but rather is an independent component that was trapped with or without mineral phases. The extreme heterogeneity in alkali contents, and in particular Rb and Sr contents, also suggests precipitation and mixing of solid precursors. The most Rb-rich glasses have near-chondritic Rb/Sr ratios, possibly indicating a chondritic source for their precursor(s). None of the inclusions contain bubbles like those of typical melt inclusions in terrestrial igneous minerals. Furthermore, many inclusions are at the center of radial cracks in the host olivine, which indicates development of an overpressure within the inclusions at some time. A volume increase of the inclusions could have been achieved by differential thermal expansion of the content of the inclusion during a heating event. That mechanism requires bubble-free and solid preheating inclusion contents. These features are incompatible with an origin of the inclusions by trapping of a silicate melt and point toward heterogeneous trapping of solid phases. The first N analyses performed in Chassigny glass-bearing inclusions by nuclear reaction analysis (NRA) revealed high and variable N contents of the glass, which suggests trapping of a solid precursor (presumably at relatively low temperatures) from a fluid rather than a melt. In conclusion, the glass-bearing inclusions in Chassigny olivine are not residuals after a closed-system evolution of a trapped melt, but rather heterogeneously trapped precipitates of a fluid that existed during formation of Chassigny constituents. Consequently, it is very unlikely that the host olivine has an igneous origin.

INTRODUCTION

The Chassigny achondrite is a member of the Shergotty–Nakhla–Chassigny (SNC) group, which is generally believed to originate from Mars (Wood and Ashwal, 1981; Bogard and Johnson, 1983; McSween, 1985). It is believed to be a cumulate rock (dunite) consisting of Fe-rich olivine (Fo_{68}) that contains glassy and partially crystallized melt inclusions (*e.g.*, Boynton *et al.*, 1976; Floran *et al.*, 1978; Johnson *et al.*, 1991; Wadhwa and Crozaz, 1995; Righter *et al.*, 1997).

Multiphase melt inclusions have been extensively studied in Chassigny (Floran *et al.*, 1978; Johnson *et al.*, 1991; Righter *et al.*, 1997, 1998) with the goal of decoding the petrogenetic history of SNC meteorites in general, and as a key to deduce the composition of the melt from which Chassigny possibly formed. Under the assumption that Chassigny is an igneous cumulate rock and the glass-bearing inclusions in the olivine represent the parental magma, Johnson *et al.* (1991) concluded that the initial trapped melt resembles terrestrial boninite lavas with ~1.5 wt% H_2O.

Other attempts to characterize the parent magma of the SNC meteorites (Shergotty and Zagami: Stolper and McSween, 1979; Nakhla: Treiman, 1986, 1990, 1993; Longhi and Pan, 1989; Harvey and McSween, 1991, 1992) have been made. These studies reached the conclusion that the parental magma for the SNC meteorites must have been similar in composition to that of terrestrial tholeiitic magmas (but somewhat poorer in Al_2O_3). Thus, the studies of Chassigny on one side and of other SNC meteorites on the other side produced conflicting results with silica-undersaturated magmas (tholeiite) producing pyroxenites (Nakhla) and silica-saturated basalts (Shergotty, *etc.*) and a silica-oversaturated magma producing a dunite (Chassigny).

Glass-bearing inclusions in SNC meteorites are generally believed to be residuals of the parental melt that was trapped during growth of the host from the melt. According to that model, subsequent "closed-system cooling" of these inclusions produced an assemblage of "daughter phases" and quenched glass. This model assumption unfortunately has led to the exclusion of inclusions smaller than 25–30 μm from the studies because they cannot be considered to be representative samples of the host melt. However, we believe that they can give us important information on the growth conditions of the host and, therefore, should not be neglected.

Here we report on the study of all three types of glass-bearing inclusions present in Chassigny olivine: pure glass, monocrystal, and multiphase inclusions. In order to tackle the question of the

origin of all inclusions and the host, we present results on the first heating experiments performed on these inclusions, detailed phase analyses, first *in situ* N analyses, and some trace element data. Our data points toward a genetic model for the Chassigny dunite that is radically different from the standard SNC meteorite model.

ANALYTICAL TECHNIQUES

Major element compositions of glasses were measured with a Camebax CAMECA electron microprobe (Centre d'analyses Camparis, Université de Paris VI) using an accelerating voltage of 15 kV and a sample current of 10 nA. A defocused beam (5–7 μm) or scanning areas of 10×10 and 15×15 μm were applied for glasses, whereas a focused beam was used for minerals. In order to reduce loss of Na during analysis, this element was analyzed first with a counting time of 5 s. For Cl and S measurements, the counting times were increased to 20 s. At the operating conditions chosen, the error for the Cl and S determinations was calculated to be between 10 and 20%. The precision for the Na, Cl, and S measurements was established by replicate analyses of basaltic and rhyolitic glasses.

Analytical scanning electron microscopy was performed with a JEOL-6400 instrument (Naturhistorisches Museum, Vienna), with a sample current of 1 nA and an acceleration voltage of 15 kV.

Proton-induced x-ray emission (PIXE) analyses were performed at the Laboratoire Pierre Süe, Saclay, France. This nondestructive technique allows *in situ* multi-element analysis with a small microbeam resolution. The operating conditions were proton beam energies of 1.7 and 3.5 MeV, a total accumulated charge of 0.4 μC, a beam current of 1.1 nA, a spot beam size of about 10×10 μm^2, and counting times ranging from 300 to 400 s. A 30 μm (for 1.7 MeV) and 100 μm (for 3.5 MeV) mylar foil was positioned in front of the x-ray detector in order to attenuate low-energy x-rays.

Nitrogen analyses were also performed at the Laboratory Pierre Süe, Saclay, France. Nitrogen-14 was detected through the nuclear reaction ^{14}N(d, p$_0$) ^{15}N with a deuteron energy of 2.1 MeV (Mosbah *et al.*, 1993). Operating conditions were a beam spot area of 5×5 μm^2, a beam current of ~0.5 nA, a total charge of 0.5 μC, and an Al screen of 9 μm thickness in front of the surface barrier detector. Titanium nitride (TiN) and a standard glass with 3.58 ($\pm$0.35) wt% N (Y$_{0.12}$Mg$_{0.16}$Si$_{0.41}$Al$_{0.30}$O$_{1.4}$N$_{0.15}$, provided by the Laboratoire de Chimie des Matériaux, Rennes I University, France) has been used for calibration. The N content of the standard glass as measured by NRA is 3.3 ($\pm$0.15) wt%.

Glass inclusions exposed on both sides of the thin section with a total depth varying between 35 and 40 μm were selected for micro-PIXE and N analyses. The main objective in selecting these types of inclusions is to avoid interference from the host olivine. The scarcity of inclusions that fulfill these conditions severely limits the number of analyses.

For the N determination, the maximum range of the beam is ~28 μm, which is less than the thickness of the inclusion. Signals from the resin and the glass were subtracted.

Heating experiments were performed in a Pt–Pt90 Rh10 heating stage at 1 bar pressure in a hot He atmosphere as O getter (Zapunnyy *et al.*, 1989). The O fugacity is estimated to have been between 10^{-9} and 10^{-10} at 1200 °C corresponding, approximately, to the equilibrium of a mixture of Ar–H$_2$ (1% H$_2$). Quenching times were <1 s. The system was calibrated at the melting point of Au (1063 °C).

RESULTS

Petrography of the Rock

The Chassigny achondrite consists of Fe-rich olivine (Fo$_{68}$) with undulatory extinction, abundant irregular fractures and glass-bearing inclusions, and a few dispersed low-Ca pyroxene (Fs$_{77}$) and chromite grains. The rock has a medium grain size (1–1.5 mm) and an equigranular texture. Most olivines are anhedral but some show crystal faces. Glass-bearing inclusions (10–150 μm) in olivine are surrounded by radial cracks. The rock is dense with only a few channel-like pores present.

Petrography of Glass Inclusions

Three types of glass-bearing inclusions are present in olivines of the Chassigny samples L6101, CHASS1, CHASS2, and CHASS3 (the latter three from sample number A 276, Naturhistorisches Museum, Vienna): pure glass, monocrystal (glass plus a crystal), and multiphase (glass plus several minerals) inclusions.

The pure glass inclusions have sizes varying from less than 10 to 40 μm in diameter, have a subrounded shape, and generally occur in clusters with a few of them being isolated in the center of some olivine grains (Fig. 1a).

Multiphase inclusions have variable sizes (nearly all >20 μm, up to 150 μm in diameter), a subrounded or euhedral (negative crystal) shape, and generally one or two of them are present in a given olivine, and only few are forming clusters. They consist of glass plus micrometer-sized crystals of low-Ca pyroxene, high-Ca pyroxene, kaersutite, chlorapatite, and troilite. Small (<20 μm) multiphase inclusions hosted by the same olivine are less abundant (Fig. 1b). Multiphase inclusions commonly contain single grains of each of the minerals listed above, but some contain only low-Ca pyroxenes.

Monocrystal inclusions consist of a single euhedral low-Ca pyroxene plus glass or a chromite plus glass and, in some of them, few needles of chlorapatite are also present. In these inclusions, the crystal–olivine contact lacks the typical curved interface but rather forms a straight (crystal face) boundary with the host olivine (Fig. 1c–d).

Pure glass and multiphase inclusions can be present in a single olivine grain. Also, multiphase and monocrystal inclusions with similar sizes and with glasses occupying highly different proportions of the inclusion cavity can occur together in the center of a given olivine grain (Fig. 1e).

Round glass-rich inclusions with some fine-grained phases are also present in the center of some chromites (Fig. 1f). Their identification is only possible in reflected light, which does not allow the detection of phases below the surface of the inclusion.

Crystals inside the inclusions are rich in irregular fractures, whereas the coexisting glass is free of fractures. The host crystals (olivine and chromite) always have well-developed radial cracks surrounding all types of inclusions. A feature common to all glass-bearing inclusions is the absence of bubbles.

Chemical Composition of Inclusion Phases

Glass–Representative glass compositions in pure glass, monocrystal, and multiphase inclusions are given in Table 1. All glasses are rich in SiO$_2$ (64–92 wt%), Al$_2$O$_3$ (16–20 wt%), Na$_2$O (1.6–11 wt%), K$_2$O (0.8–6 wt%), and Cl (1500–5200 ppm), and poor in MgO (<2 wt%), FeO (<1.5 wt%), and CaO (<1.5 wt%).

Pure glass inclusions are dominated by highly quartz-normative compositions that, however, range toward and overlap with compo-
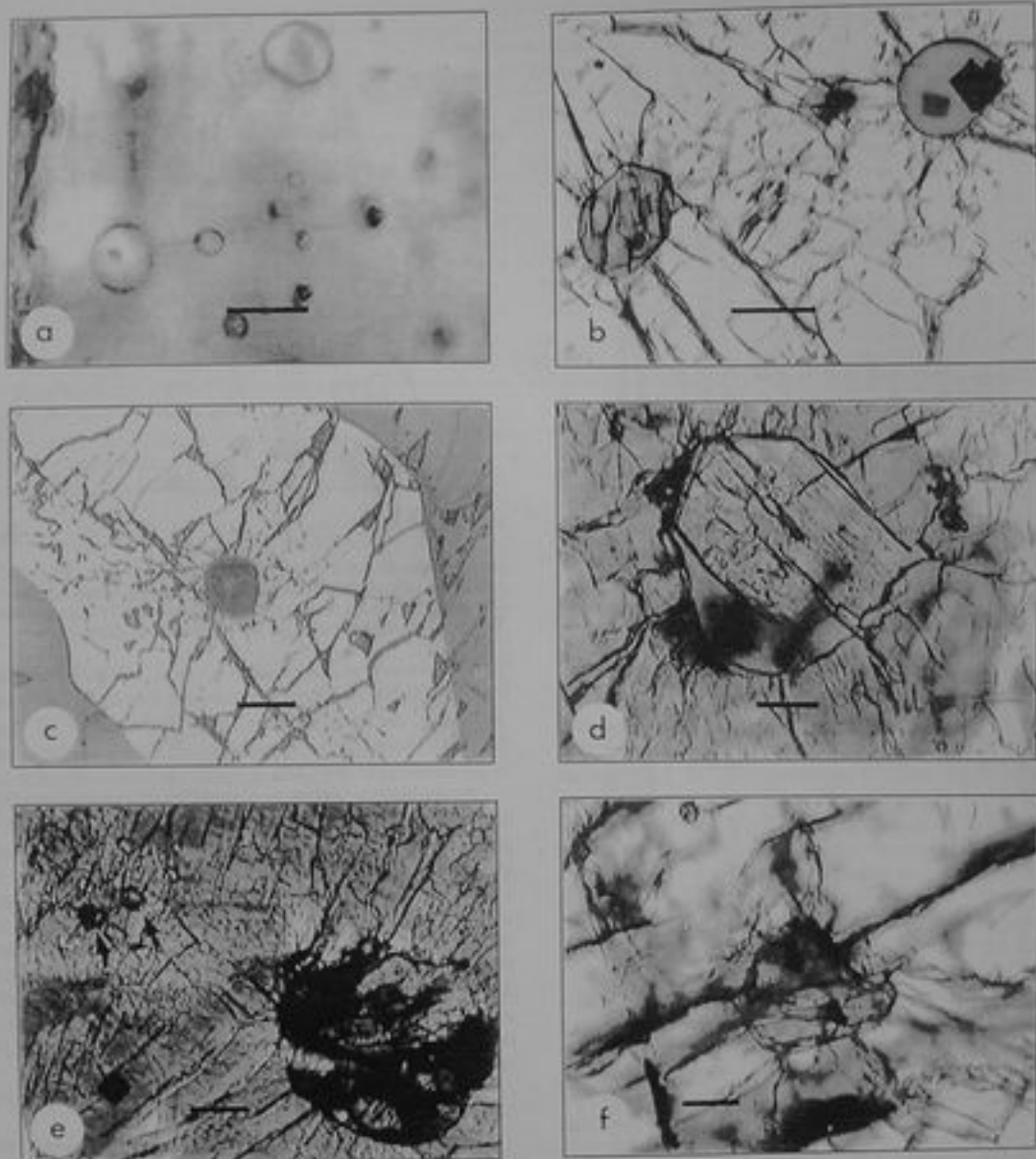
sitions of glass in multiphase inclusions (Fig. 3). Glasses of pure glass inclusions have similar major element contents as glasses from other inclusions but have somewhat restricted variations in the contents of CaO (0.2–0.7 wt%), Na_2O (0.9–8.4 wt%), and K_2O (0.5–5.6 wt%) (Fig. 2). Inclusions of very different sizes present in the same host mineral have similar glass compositions (e.g., inclusion CH2 is double in size compared to inclusion CH1, note

the similar Na_2O and K_2O contents, Table 1). Glasses in inclusions decorating fractures (CH3 and CH4, Table 1) or present as clusters in different host olivines are Na_2O-poor with no variation in alkali contents but highly variable contents of Cl (e.g., 1400 and 4900 ppm, respectively). Only in one cluster, coexisting inclusions poor and rich in Na_2O were found. Isolated inclusions that occur in the center of olivine grains have similar major element contents and

TABLE 1. Selected representative EMP analyses (wt%) of glass in inclusions in chassigny olivine

	CH1	CH2	CH3	CH4	CH5	CH6	CH7	CH8	CH10	CH10	CH*	CH*	CH*	CH*	CH*	CHa	CHa	CH9	CH10	CH12
SiO_2	71.2	72.9	78.6	76.1	71.5	72.6	70.3	71.6	71.2	70.5	70.4	70.5	63.9	71.0	70.2	78.6	92.2	69.9	71.1	70.0
TiO_2	0.30	0.14	0.18	0.05	0.16	0.19	0.16	0.31	0.25	0.19	0.28	0.34	0.08	0.22	0.24	0.24	0.16	0.15	0.12	0.20
Al_2O_3	16.9	16.2	17.4	17.1	15.8	16.8	16.7	16.8	17.3	17.1	17.4	17.1	19.8	16.7	16.4	11.9	3.68	17.5	16.4	16.8
FeO	1.02	0.98	1.09	1.94	0.65	0.79	0.63	0.72	0.66	0.59	0.91	0.82	0.41	0.62	0.66	0.76	0.29	1.19	2.08	3.28
MnO	0.00	0.11	0.00	0.02	0.15	0.00	0.04	0.08	0.00	0.00	0.08	0.00	0.01	0.03	0.07	0.00	0.09	0.06	0.04	0.10
MgO	0.01	0.03	0.07	0.07	0.18	0.03	0.03	0.05	0.04	0.04	0.03	0.03	0.04	0.01	0.04	0.06	0.91	0.83	0.51	1.16
CaO	0.34	0.38	0.76	0.77	0.23	0.18	0.33	0.77	0.90	0.55	0.38	0.88	1.46	0.54	0.45	0.14	0.11	0.81	1.24	1.31
Na_2O	8.4	7.7	1.10	1.65	5.8	7.9	6.6	8.3	6.8	8.6	8.5	7.5	7.4	8.1	8.4	2.77	0.88	3.7	3.8	3.6
K_2O	1.94	1.97	0.80	1.30	5.6	2.21	4.4	1.47	1.63	1.97	1.87	1.69	5.9	2.17	1.87	3.8	0.43	4.5	4.1	3.2
Total	100.1	100.4	100.0	99.0	100.0	100.7	99.2	100.1	98.7	99.5	99.9	98.9	99.1	99.4	98.4	98.3	98.7	98.7	99.4	99.7
Cl (ppm)	3040	4200	1400	4600	3400	4900	3000	5200	1900	3020	3490	2330	3860	3650	1950	1860	260	–	–	–
	(12)	(25)	(10)	(10)	(20)	(20)	(40)	(50)	(50)	(30)	(40)	(60)	(150)	(30)	(50)	(20)	(20)	(20–70)	(20–30)	(40–70)

CH = pure glass inclusions; CH* = glass in multiphase inclusions; CHa = glass in inclusions in chromite; CH9 = mean glass composition of seven inclusions heated to 1200 °C; CH10 = mean glass composition of six inclusions heated to 1000 °C; CH12 = mean glass composition of six inclusions heated to 900 °C; – = <100 ppm. Numbers in parentheses represent the apparent size (20) or range of sizes (20–40) of the inclusions in micrometers.
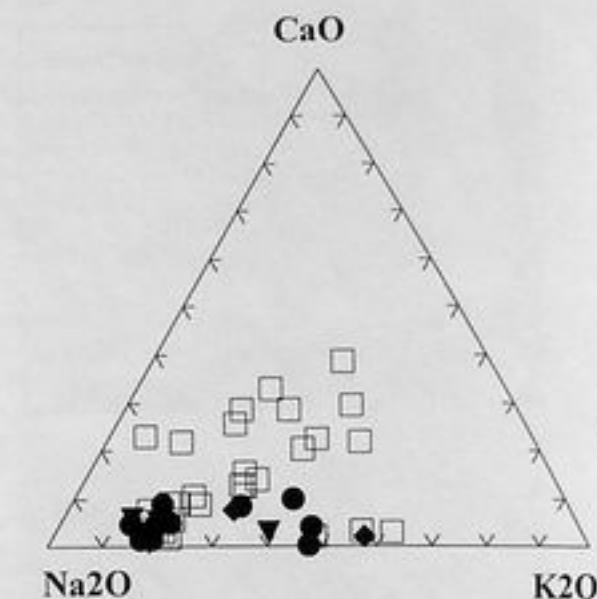

FIG. 2. Projection contents (in wt%) of CaO–Na₂O–K₂O in glass of unheated pure glass, monocrystalline, and multiphase inclusions in the olivine of Chassigny. Symbols: ● = multiphase inclusions; □ = pure glass inclusions; ▼ = monocrystalline inclusions; ◆ = inclusions in chromite.

variable contents of Na_2O and K_2O (e.g., compare inclusions CH5 and CH6, Table 1). The same chemical variation is observed when comparing the isolated pure glass inclusions CH7 and CH8 (Table 1). Note that these inclusions are double in size as compared to inclusions CH5 and CH6.

All multiphase inclusions contain Na_2O-rich glasses (Na_2O, 7.1 to 12.6 wt%; Tables 1 and 2, Fig. 2). Inclusions with similar glass/crystal (e.g., low-Ca pyroxene, clinopyroxene) ratios have glasses with similarly high contents of Na_2O but highly different contents of K_2O (see Glass1 and Glass2, Table 2). One multiphase inclusion that contains low-Ca pyroxene, clinopyroxene, kaersutite and chromite has glass of two different chemical compositions (e.g., Na_2O, K_2O, and Cl) (Table 2). Normative mineral compositions are dominated by albite with a tendency towards increasing orthoclase contents (Fig. 3). The most K-rich glasses have been found in multiphase inclusions containing up to 6.9 wt% K_2O that corresponds to >40% normative orthoclase (Fig. 3).

Glasses from monocrystal inclusions are very Na_2O-rich (7–10 wt%) with K_2O contents <2.5 wt%.

Glasses of inclusions in chromite are very silica-rich, showing the highest contents in SiO_2 of all monocrystal and multiphase inclusions (Table 1).

The abundances of some minor and trace elements in the glass of inclusions as obtained by EMP, micro-PIXE, and NRA analyses are given in Table 3. The Rb and Sr contents vary from 8 to 210 ppm and 200 to 940 ppm, respectively. The N contents are also highly variable and range from 160 to 7450 ppm. The contents increase with depth from the section's surface (Table 3).

Minerals—The chemical composition of the main phase olivine is constant throughout the rock. It is FeO-rich (Fa_{32}) and rich in CaO (0.09–0.22 wt%). Low-Ca pyroxene is rich in CaO (1.3 wt%), TiO_2 (0.17 wt%), Cr_2O_3 (0.23 wt%), and Al_2O_3 (0.7 wt%) (Table 2). Calcium-rich pyroxene is rich in TiO_2 (0.5–0.9 wt%), Al_2O_3 (4–10 wt%), and Na_2O (0.5–1.3 wt%), but fairly poor in

TABLE 2. Representative analyses of coexisting phases and glasses in multiphase and monocrystalline inclusions.

	Multiphase inclusions														
	Opx	Kaer	Kaer	Cpx	Cr	Opx	Glass*	Glass*	Opx	Cpx	Glass1	Glass2	Opx	Opx	Glass
SiO$_2$	52.3	39.4	39.0	50.4	0.07	52.3	64.2	64.2	54.5	49.1	70.4	64.5	53.1	53.0	63.2
TiO$_2$	0.47	7.20	6.20	0.94	3.39	0.44	0.08	0.06	0.29	0.46	0.28	0.26	0.55	0.51	0.08
Al$_2$O$_3$	2.78	13.4	12.9	4.0	12.9	3.2	20.8	22.3	1.59	9.6	17.4	19.6	3.00	3.5	21.4
Cr$_2$O$_3$	0.28	0.77	0.68	0.48	45.2	0.34	0.05	0.00	0.15	0.14	0.00	0.00	0.53	0.25	0.00
FeO	17.0	10.1	9.90	8.6	32.9	16.8	0.59	0.52	14.8	6.4	0.91	0.31	15.3	16.2	0.87
MnO	0.59	0.23	0.37	0.36	0.53	0.48	0.02	0.00	0.52	0.15	0.08	0.00	0.41	0.46	0.01
MgO	24.5	11.3	11.6	14.8	3.94	24.7	0.02	0.02	25.3	11.4	0.03	0.03	23.4	24.8	0.03
CaO	1.93	10.9	10.4	19.2	0.03	1.58	0.04	0.28	3.73	20.7	0.37	1.56	3.6	0.97	0.06
Na$_2$O	0.06	3.20	3.10	0.45	0.00	0.06	7.6	12.6	0.09	1.29	8.5	7.5	0.29	0.11	7.1
K$_2$O	0.05	0.24	0.21	0.00	0.00	0.00	6.9	0.25	0.00	0.00	1.87	5.9	0.01	0.06	6.6
Total	99.7	96.7	94.4	99.3	98.9	99.9	100.3	100.2	100.9	99.3	99.9	99.6	100.2	99.8	99.3
Cl ppm	-	1700	2200	-	-	-	3790	410	-	-	3490	3720	-	-	1280

	Monocrystalline inclusions				
	Opx	Glass	Opx†	Cr	Glass
SiO$_2$	53.1	63.9	53.8	-	70.3
TiO$_2$	0.26	0.06	0.17	4.5	0.24
Al$_2$O$_3$	0.75	20.9	0.74	7.7	17.0
Cr$_2$O$_3$	0.11	0.06	0.23	46.5	0.01
FeO	16.5	0.45	18.0	37.1	0.82
MnO	0.54	0.00	0.59	0.60	0.06
MgO	26.6	0.02	24.5	2.75	0.02
CaO	1.06	0.12	1.30	0.02	0.67
Na$_2$O	0.06	10.9	0.04	-	9.50
K$_2$O	0.02	2.4	n.d	-	1.50
Total	99.0	98.8	99.4	99.2	100.1
Cl ppm	-	3260	-	-	2080

*Glasses in the same multiphase inclusion.
†Orthopyroxene cumulus phase (Floran et al., 1978).
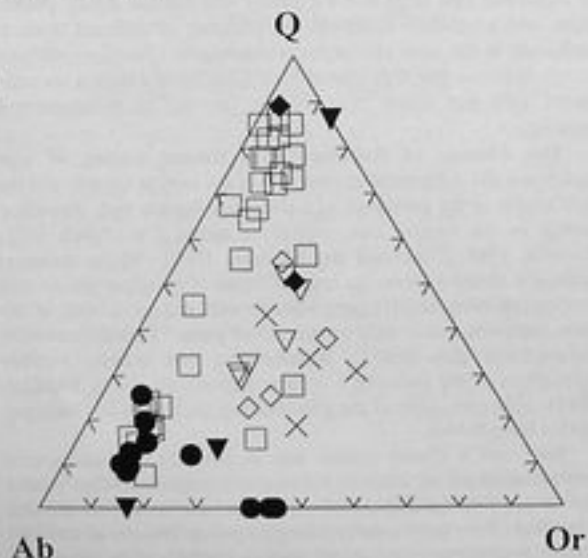n.d. = not determined

Q

Ab

Or

FIG. 3. Normative composition of glass in pure glass, monocrystalline, and multiphase unheated and heated inclusions. Symbols: ● = multiphase inclusions; □ = pure glass inclusions; ▼ = monocrystalline inclusions; ◆ = inclusions in chromite; × = heated inclusions (900 °C); ◇ = heated inclusions (1000 °C); ∇ = heated inclusions (1200 °C).

Cr_2O_3 (0.1–0.5 wt%). Chromite is MgO-poor (3–4 wt%) and rich in TiO_2 (3.4–4.5 wt%) and Al_2O_3 (8–13 wt%).

Low-Ca pyroxene in monocrystal inclusions has a composition similar to that of the rock-forming pyroxene. All phases of multiphase inclusions have variable compositions (Table 2). Low-Ca pyroxene in multiphase inclusions, for example, has a composition different from that of the rock-forming pyroxene with high and variable TiO_2 (0.29–0.55 wt%), Al_2O_3 (1.59–3 wt%), and CaO (1.93–3.73 wt%) contents.

Heating Experiments

Several heating experiments have been performed on the Chassigny samples with varying heating rates from 5 °C/min up to 20 °C/min. One of the first problems we faced was the darkening of the samples. In all experiments, fractures began to get dark at temperatures of ~300 °C. This darkening intensified at high temperatures (~450 °C) and, due mainly to the high abundance of fractures in the olivine, the sample became completely dark. All heated samples showed the same behavior that was independent of the heating rate. At temperatures between 900 and 1000 °C, samples gradually became clear. Experiments performed with a low heating rate (up to 1100 °C) and that were held for an additional 12 h at this final temperature caused a complete darkening of the sample despite the operating conditions chosen (heated He atmosphere as O getter). Possibly, the He flux was not large enough to prevent the sample from total oxidation.

Another problem to solve was that of decrepitation of inclusions at relatively low temperatures mainly due to the presence of radiating fractures around the inclusions. The experiments undertaken at heating rates of 10–15 °C/min showed that total decrepitation of inclusions occurred at temperatures <1100 °C. Runs of ~8 h each with heating rates of 5 °C/min up to 300 °C, 2–3 °C/min up to 700 °C, and 1–2 °C/min from this temperature up to the final temperature of 900, 1000, and 1200 °C, respectively, appear to be the optimum conditions that prevent both a total darkening and an early decrepitation of the inclusions. The final temperatures were held for 30 min after which a rapid quench (<1 s to ~500 °C) preserved the final conditions and prevented crystallization of the melt. After these experiments, the chemical composition of the glass was determined. It turned out that the chemical composition of the glass in the heated inclusions (Table 4) varies somewhat (in wt%): SiO_2 (65–74), Al_2O_3 (15–22), FeO (0.6–5.4), CaO (0.5–1.7), Na_2O (2.4–5), and K_2O (2.7–6). Normative compositions of these glasses are shown in Fig. 3.

TABLE 3. Micro-PIXE and nuclear reaction analysis of glass inclusions in sample L6101 (in wt%).

Inclusion		128	130	132	125	122	IG
TiO_2	EMP	0.22	0.20	0.25	0.19	0.16	0.08
	PIXE	0.25	0.22	0.27	0.19	0.21	0.14
CaO	EMP	0.54	0.55	0.97	0.12	0.34	1.46
	PIXE	0.65	0.78	1.64	0.71	0.57	1.10
K_2O	EMP	2.17	1.97	3.6	2.46	4.4	5.9
	PIXE	2.63	2.63	4.5	2.68	4.3	7.0
Cl (ppm)	EMP	3650	3000	3100	3300	2900	3860
	PIXE	4200	3600	4100	4300	3800	3960
Rb (ppm)	PIXE	8	24	57	20	150	210
Sr (ppm)	PIXE	559	680	800	200	800	940
N (ppm)	NRA	–	880	–	160	543	273
		–	(0–14)	–	(0–6)	(0–28)	(0–19)
		–	4200	–	4780	–	2200
		–	(14–28)	–	(6–14)	–	(19–24)
		–	–	–	7450	–	–
		–	–	–	(14–28)	–	–

Inclusions of sample L6101: 128, 132, 125, 122, and IG have 30–35 μm depth and are exposed on both sides of the thin section. Monocrystalline inclusions: 122, 125, and 130; multiphase inclusions: 128, 132, and IG. Number in parenthesis corresponds to the depth from which the data came.

DISCUSSION

Previous Works

The Chassigny achondrite consists of Fe-rich olivine (Fo_{68}) with anhedral to euhedral shape that is suggestive of a cumulate origin (Floran et al., 1978). According to these authors, pyroxene can also be considered a cumulus phase, and its chemical composition (e.g., Fe/(Fe + Mg) ratio) compared to that of olivine has been considered to be consistent with a cogenetic origin. The texture and mineralogy indicate that Chassigny is a recrystallized cumulate dunite which possibly formed from a fractionated melt rather than a residual rock after partial melting (Prinz et al., 1974). Mason et al. (1975) suggested that Chassigny is an olivine-rich cumulate derived from a chondrite-like magma. The magma from which Chassigny is supposed to have formed must have been highly enriched in the light rare earth elements (Boynton et al., 1976; Wadhwa and Crozaz, 1995). According to Boynton et al. (1976), the similarity in the fractionated REE patterns of Chassigny and the nakhlites suggests a genetic relationship. However, the distribution of the trace and minor elements in augites, nakhlites, and Chassigny suggest that the latter was not comagmatic with nakhlites (Wadhwa and Crozaz, 1995). According to Stolper et al. (1979), the source regions of the parent magmas of these rocks (the basaltic shergottites, the pyroxenitic nakhlites, and the dunite Chassigny), although clearly distinct, seem to be related by mixtures of volatile-rich and volatile-poor components in planetary or nebular settings or by volatile loss from an originally volatile-rich primitive material.

Notwithstanding the extensive works done to characterize the composition of the parent magma of the SNC meteorites, this still remains a matter of debate, as are also the origins of olivine and augite in nakhlites because these two minerals are not in Fe/Mg equilibrium (e.g., Bunch and Reid, 1975; Nakamura et al., 1982; Treiman, 1986). A summary of current hypotheses on the genesis of SNC meteorites in general, and on Chassigny in particular, can be found in McSween (1994).

Particular Features of the Glass-bearing Inclusions in Chassigny Olivine

Inclusion Sizes–Previous work on Chassigny melt inclusions (Johnson et al., 1991) only considered large inclusions that are all multiphase inclusions. However, in the samples studied by us, some multiphase inclusions have similarly small sizes than pure glass inclusions.

To examine the problem of inclusions' size, we have studied glass inclusions in olivine of Sommata (Vulcano, Eolian Island) lavas that have a composition close to boninite with 2–4 % H_2O (Gioncada et al., unpubl. data) and thus, also close to that proposed for the parental magma of Chassigny (Johnson et al., 1991). Also, and considering that in Chassigny inclusions with different sizes are trapped in the same host, we have chosen two glass inclusions of very different sizes hosted in the same olivine for the heating experiments. The temperature was raised to 1150 °C. This temperature is close to the homogenization temperature and thus to the liquidus of the inclusion (Sobolev and Nikossian, 1994). While lowering the temperature from 1150 °C to room temperature, daughter crystals have nucleated in both types of inclusions (e.g., clinopyroxene and phlogopite). In the large and the small inclusion, the daughter crystals and a bubble occupied approximately 50 and 30% of the inclusions' cavity, respectively. This experiment shows that if small and large inclusions that are hosted by the same olivine sampled the same ambient liquid and resulted from a closed-system cooling, they will evolve in a very similar way. This example maintains our belief that the study of inclusions with different sizes will help to give a complete spectrum of the conditions prevailing during their formation.

If the same cooling rate is applied, as in our example, both types of inclusions (the large and the small) will contain crystal phases, glass, and a bubble. However, the presence of different types of inclusions in the same olivine, as is common in Chassigny olivines, clearly indicates that they cannot have been formed from a common parent melt but rather must be the product of heterogeneous trapping.

The Absence of Bubbles–During natural cooling of melt inclusions, the differential contraction of the host (a crystal) and the melt results in the formation of a shrinkage bubble and, depending mainly on the cooling rate, crystalline nuclei (Clocchiatti, 1975; Roedder, 1984; Clocchiatti and Massare, 1985). If the inclusion remains a closed system, the crystallization of daughter phases will produce an even larger empty volume with respect to that of the same inclusion that is only composed of glass. This difference in volume will give rise to bubbles that can occupy variable proportions of the inclusion's volume (Clocchiatti, 1975; Roedder, 1984). However, none of the glass-bearing inclusions in Chassigny olivine has a bubble.

How can a closed system that evolved by post-entrapment crystallization of an initially volatile-rich magma develop phases that occupy 50% (or more) of the inclusion's cavity without forming a bubble? We cannot invoke a single cooling process of a closed system accompanied by post-entrapment crystallization because, if this is the case, the system would have had to develop a bubble.

Possible Mechanisms

Shock Pressure and Quenching–One possible solution is to consider that the inclusions were originally composed of glass plus

TABLE 4. Representative EMP analyses of phases in heated inclusions.

Final temperature 900 °C

	Multiphase inclusions						Pure glass inclusions		
	Opx	Cpx	Opx	Cpx	Glass	Host	Glass	Glass	Host
SiO_2	52.8	50.2	53.1	51.3	65.8	36.9	70.6	73.7	37.7
TiO_2	0.32	1.29	0.21	1.12	0.12	0.02	0.03	0.11	0.02
Al_2O_3	3.2	4.7	3.1	8.2	21.9	0.04	16.7	17.2	0.04
Cr_2O_3	0.09	0.08	0.10	0.16	0.00	0.03	0.07	0.06	0.00
FeO	16.9	8.13	16.3	6.19	0.55	27.9	1.06	0.64	26.9
MnO	0.48	0.27	0.47	0.30	0.06	0.05	0.08	0.01	0.58
MgO	24.7	14.5	24.2	11.2	0.09	33.9	0.14	0.13	34.4
CaO	1.18	19.3	1.51	19.5	0.52	0.22	0.78	0.59	0.18
Na_2O	0.08	0.59	0.11	0.79	4.4	–	5.1	3.6	–
K_2O	0.08	0.14	0.16	0.08	6.1	–	4.8	3.3	–
Total	99.9	99.2	99.2	98.8	99.6	99.1	99.4	99.4	99.8

Final temperature 1000 °C

	Pure glass inclusions				
	Glass	Host	Glass	Glass	Host
SiO_2	71.4	37.6	70.3	73.4	35.9
TiO_2	0.03	0.02	0.15	0.17	0.00
Al_2O_3	16.0	0.01	16.51	15.6	0.00
Cr_2O_3	0.00	0.04	0.00	0.02	0.01
FeO	2.54	28.5	1.64	1.75	28.1
MnO	0.14	0.65	0.00	0.00	0.48
MgO	0.86	33.9	0.35	0.26	34.6
CaO	1.46	0.08	0.97	1.03	0.16
Na_2O	2.50	0.00	5.1	3.4	0.00
K_2O	5.0	0.03	4.3	2.72	0.00
Total	99.9	100.8	99.3	98.4	99.3

Final temperature 1200 °C

	Multiphase inclusions						Pure glass inclusions		
	Ol1	Glass1	Ol2	Opx2	Glass2	Host	Glass	Glass	Host
SiO_2	37.7	69.1	37.4	54.8	70.1	37.1	71.9	69.3	37.2
TiO_2	0.08	0.12	0.00	0.05	0.17	0.09	0.22	0.25	0.19
Al_2O_3	0.19	16.7	0.00	1.07	18.2	0.00	17.2	16.3	0.00
Cr_2O_3	0.00	0.00	0.26	0.00	0.06	0.00	0.00	0.00	0.00
FeO	29.2	3.12	29.8	16.9	3.19	29.8	2.23	3.71	29.2
MnO	0.48	0.07	0.13	0.68	0.08	0.51	0.13	0.05	0.71
MgO	32.5	1.32	31.3	25.9	0.79	32.9	0.57	0.97	32.9
CaO	0.01	1.24	0.19	0.60	1.31	0.16	1.13	1.37	0.12
Na_2O	0.06	4.11	0.41	0.05	2.35	–	4.0	4.4	–
K_2O	0.02	3.3	0.00	0.13	2.81	–	3.2	3.3	–
Total	100.2	99.1	99.5	99.6	99.1	100.4	100.5	99.7	100.3

crystals plus bubble and, as a result of shock pressures on the order of 150–200 kbar that this meteorite is believed to have suffered (Floran et al., 1978), the glass of the inclusions was shock melted (Johnson et al., 1991) and then rapidly quenched without leaving the system the time to develop a bubble. The planar and irregular fractures in the olivine have been considered evidence for this shock event (Floran et al., 1978). If the glass of the inclusions was melted in such an event, it would be very likely that this melt penetrated the surrounding fractures. Therefore, the inclusions would not be closed systems as they would have lost part of the melt and, thus, their chemical composition cannot be representative of the initial melt. However, there is no trace of glass in the fractures (in contrast to what has been described from the Shergotty achondrite—e.g., El Goresy et al., 1997). Therefore, formation of bubble-free inclusions and their glass by a shock melting event seems to be highly unlikely.

Heterogeneous Trapping and Quenching–Another possibility could be that the inclusions were formed by heterogeneous trapping of a melt (plus preexistent minerals) that was rapidly quenched before the cracks were formed. This could explain the absence of a bubble in multiphase and monocrystal inclusions and the absence of a shrinkage bubble in pure glass inclusions. The trouble is: How can one grow and accumulate large crystals, compositionally homogenize them, and quickly cool the system at the same time?

Metastability–Inclusions that have trapped melt rich in volatiles will generally nucleate a bubble during cooling, but some melt inclusions will not. This lack of phase change within inclusions after they have been trapped can be explained in terms of metastability (Roedder, 1984). According to that author, "significant degrees of metastability (usually stated in the term of temperature) are most commonly encountered in the nucleation of gas bubble and daughter minerals on cooling inclusions that were previously homogeneous." Three main factors, extensively explained by Roedder (1979, 1984) can be responsible for the suppression of bubbles. All three depend on the size of the inclusion. According to Roedder (1979), and as a result of this size effect, generally only the larger inclusions in a given sample will have bubbles. Again, this is not the case in Chassigny where all inclusions, the big and the small, lack bubbles.

Low Contents of Volatiles in the Melt–The presence or absence of a bubble in a glass inclusions could also be related to the contents of volatiles in the melt. The presence of amphibole in the inclusions were taken as evidence for "volatile-bearing" inclusions (Johnson et al., 1991; Harvey and McSween, 1992). However, many of the kaersutites present in SNC meteorites are oxy-kaersutites and are stable under dry conditions (Watson et al., 1994). Such dry amphiboles could be in equilibrium with a melt containing only 100 to 1000 ppm H_2O (Mysen et al., 1998). Thus, this low content of volatiles could be believed not to be enough to nucleate a bubble in the melt inclusion. However, in melt inclusions of upper mantle minerals where the content of H_2O was estimated to be less than ~0.02 wt%, all glass inclusions have a shrinkage bubble (Schiano et al., 1998).

The Most Possible Mechanism–The only way the absence of bubbles can be explained in all types of inclusions is that a differential shrinkage between the melt and the host has never occurred. This would imply a fairly low temperature during the process of trapping and, consequently, during the growth of the host.

So, we are left with the possibility that the glass (or a crystalline precursor) was trapped together with the minerals and carrier phases of the trace elements (heterogeneous trapping), and no melt was involved during the trapping event.

In the following paragraphs, we give more evidence besides that already mentioned above, which points toward the fact that glass-bearing inclusions in Chassigny can be produced by heterogeneous trapping of all its constituents at sub-igneous temperatures. Finally, a new possible mechanism for the formation of these glass-bearing inclusions is proposed that has a direct repercussion on the petrogenetic scenario of this rock.

Heterogeneous Trapping

Petrography of Glass-bearing Inclusions–Low-Ca pyroxene is the most abundant and the largest crystalline phase present in glass-bearing inclusions in olivine of Chassigny. Its composition varies between about $En_{68}Fs_{25}Wo_7$ and $En_{72}Fs_{26}Wo_2$. Low-Ca pyroxene in monocrystal inclusions has a chemical composition similar to that of the low-Ca pyroxene of the Chassigny rock (Table 2). This similarity and the fact that the low-Ca pyroxene grains have euhedral contacts with the host olivine suggest that low-Ca pyroxene can be considered a preexisting phase with respect to the time of formation of the inclusions. Similar monocrystal inclusions, with augite as the dominant phase, were previously described by Harvey and McSween (1992) from the Nakhla and the Governador Valadares nakhlites.

Low-Ca pyroxenes have chemical compositions depending on their occurrence. There was no equilibration of the phases which, if it was by metamorphic reequilibration, should also have destroyed the glass.

Monocrystal glass inclusions have the highest contents of Na_2O (9.5–11 wt%) as compared to all other multiphase inclusions (Table 2). One multiphase inclusion shows two different chemical compositions of the "residual glass." These heterogeneous glasses could be explained due either to unmixing at low temperatures (Delano and Hanson, 1996) or to the presence of submicroscopic intergrowth of silica minerals and feldspar, in a similar way to that observed in shergottites (Ikeda, 1998).

As was mentioned above, monocrystal and multiphase inclusions can coexist in the center of olivine grains. Glasses in both types of inclusions occupy highly different proportions of the inclusion cavity. The mineralogy also differs from one inclusion to another. Their sizes, however, are similar. The primary nature of these inclusions indicates that they were trapped during growth of the Chassigny olivine. Thus, they are very likely representative samples of the ambient phases that existed at the time of entrapment.

If monocrystal and multiphase inclusions were trapped in different grains, we could consider that the quite distinct textures exhibited by these inclusions are indicative of different formation conditions, as has previously been noted in the Nakhla meteorite (Harvey and McSween, 1992). However, the situation in Chassigny is quite different from that in Nakhla. We cannot invoke a different formation condition that would allow us to choose one type of inclusion with respect to the other, when both have been contemporaneously trapped by the very same host. If these inclusions represent the melt and an assemblage of "daughter inclusions represent the melt and an assemblage of "daughter phases" that crystallized during subsequent closed-system cooling, as suggested by Johnson et al. (1991), then the question arises: Which igneous process has to be invoked to explain the fact that similar volumes of melt from a homogeneous reservoir, contemporaneously trapped in the same host olivine, can have so different evolutions? Is this the same process that can also explain the existence of pure glass and multiphase inclusions with similar glass compositions in the same host grain? There is no such process

and, consequently, only heterogeneous trapping (i.e., chance trapping of phases, crystalline and noncrystalline) that existed at the moment of the inclusion formation can explain this situation.

Compositional Variability of Glasses Precludes a Derivation from a Homogeneous Reservoir–The compositional variability of glasses from all inclusions is surprisingly large, and few elements have correlated abundances. The FeO and MgO contents are positively correlated (Fig. 4). This positive correlation has to be taken with care, as it is found only in pure glass and heated multiphase inclusions. Therefore, it could be the result of excitation of the inclusion's walls by primary x-rays during analysis (fluorescence) or of the heating experiments, respectively. The Na_2O and K_2O contents are negatively correlated with the SiO_2 content (Fig. 4). The decrease of the alkali contents with increasing silica is much too large for a simple dilution effect. It rather must reflect compositional differences between the sources.

The large and chaotic variability of alkalis, halogens and others in the glass inclusions precludes a derivation from a homogeneous reservoir. Glasses cannot represent the residual melt from which the olivines could possibly have grown.

In addition, glasses in multiphase inclusions with highly different quantities and proportions of minerals have variable contents of SiO_2 and similar contents of Na_2O. If glasses were the residua after crystallization in a closed system, we have to expect the mineral-rich inclusions to represent the final stage of the evolution and, thus, to have the highest contents of Na_2O. However, the highest content of Na_2O of all inclusions have glasses of monocrystal inclusions where they occupy a high-volume proportion of the inclusion and where crystal phases are close in composition to that of the minerals in the rock. This is an additional indication for heterogeneous trapping.

Furthermore, the glass composition of multiphase and pure glass inclusions is similar and has similar chaotic variability. If the parent melt is contemporaneously trapped into two inclusions in a given host phase, and some phases grow in one inclusion but not in the other, a chemical variation of the residual melt and differences in the composition of glasses from multiphase and pure glass inclusions must be expected. Such a difference exists but it is opposite to what has to be expected: pure glass inclusions have the most SiO_2-rich glass of all inclusions, despite the fact that they did not produce daughter minerals. These features could in part be due to the smallness of these inclusions because the high surface/volume ratio likely has some influence on the precipitation behavior of melts and fluids and thus can affect the chemical composition of the precipitate. Nucleation of any new phase will depend on the composition of the trapped liquid, the rate of cooling, and the nature of the host mineral (Roedder, 1979). However, the fact that small inclusions were formed rather than big ones must be a consequence of the local conditions.

In summary, the compositional variability observed in glass-bearing inclusions could indicate that olivines have heterogeneously sampled phases in varying proportions. Consequently, these phases must have been present during growth of the olivine. The large low-Ca pyroxenes that were trapped in monocrystal inclusions, relative to those in the rock, were small enough to be caught by the growing olivine. Small crystals are out of equilibrium with the large ones in a similar way to that previously observed in Nakhla. According to Treiman (1993), phases that do nucleate may grow rapidly, leading to crystals with nonequilibrium compositions. However, in Chassigny the glass precursors also seem to be out of
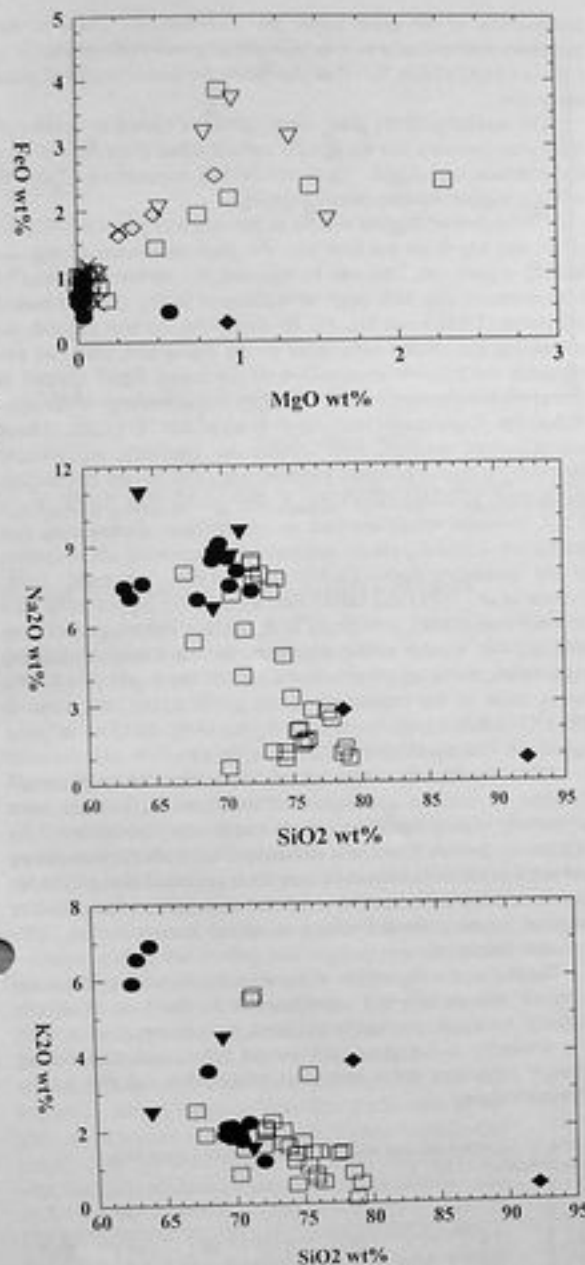
FIG 4. Compositional variation of glasses in inclusions of Chassigny olivine. (a) FeO vs. MgO; (b) Na$_2$O vs. SiO$_2$; (c) K$_2$O vs. SiO$_2$. Symbols: ● = multiphase inclusions; □ = pure glass inclusions; ▼ = monocrystalline inclusions; ◆ = inclusions in chromite; × = heated inclusions (900 °C), ◇ = heated inclusions (1000 °C); ▽ = heated inclusions (1200 °C).

equilibrium with each other. Cluster inclusions with nonhomogeneous glass compositions indicate chemically heterogeneous precursors for the glass or mixing of precursor components shortly before or during trapping. The extreme variability of the alkali and Sr contents of the glasses suggests that these elements were carried by solid precursors that were sampled in different amounts by different inclusions.

Heating Experiments Support Heterogeneous Trapping

To obtain the composition of the initial liquid of an evolved glass-bearing inclusion, we can either (1) calculate it from the mineralogy of the inclusion using a system of mass balance equations solved by linear regression methods (e.g., Johnson et al., 1991; Harvey and McSween, 1992), or (2) perform heating experiments that will allow the processes that occurred inside the inclusions during cooling to be reversed. Many heating experiments on glass-bearing inclusions as experimental crystallization have been performed to obtain information regarding the liquidus, the sequence of crystallization of different phases, and to determine the physico-chemical conditions prevailing during crystallization of the host (e.g., Sobolev and Kostyuk 1975; Sobolev et al., 1976; Clocchiatti, 1975; Clocchiatti et al., 1978; Roedder, 1984; Clocchiatti and Massare, 1985).

For the calculation of the initial liquid's composition, assumptions as to the proportions of the phases inside the inclusion and the real volume have to be made, which consequently lead to a simplification of the natural system. In the second method, the whole inclusion with all its phases (daughter phases and the layer of the host mineral crystallized onto the inclusion's walls) are treated together, as well as its host mineral. We have chosen the heating experiment in spite of the constraints imposed by the decrepitation phenomenon, the limited duration of heating runs, and the oxidation of the sample. An additional limitation to this method is the pressure conditions, as all our heating experiments were performed at 1 bar. Of particular importance is an adequate duration of the heating runs because, if they are too short, no dissolution of the daughter phases and of the host that could have crystallized after trapping will take place. If it is long, samples will oxidize. The optimum conditions during these experiments that prevented both decrepitation and oxidation have been already described (see Analytical Technique section).

During these experiments, migration of the melt to open fractures will produce empty inclusions, similar to those obtained due to decrepitation. One heating experiment was done to precisely determine the temperature referred to as decrepitation temperature. For this purpose, pure glass inclusions with few surrounding fractures were chosen. In this way, the possibility for early decrepitation is minimized. Total decrepitation (the inclusions suddenly became dark) was observed at temperatures between 1130 and 1150 °C. This decrepitation temperature is in good agreement with the "equilibration temperature" estimated from coexisting pyroxene pairs in Chassigny inclusions (Johnson et al., 1991) and with the "accumulation" temperature of 1140 °C (Stolper and McSween, 1979) estimated for Shergotty and Zagami shergottites (other members of the SNC group). Thus, at the final temperature of 1200 °C, to which some Chassigny inclusions have been heated, possible reactions and dissolution with/of the host can be expected. Nevertheless, the glass of the inclusions heated to this high temperature remained SiO$_2$-rich.

Figure 5 shows the chemical composition of glasses in an inclusion that was heated to a final temperature of 1200 °C. There is no significant variation in the Na$_2$O, K$_2$O, and CaO contents of glasses inside the inclusion and glasses filling the surrounding glasses. However, glasses filling the fractures are rich in FeO and MgO, which indicates dissolution of some host olivine. The
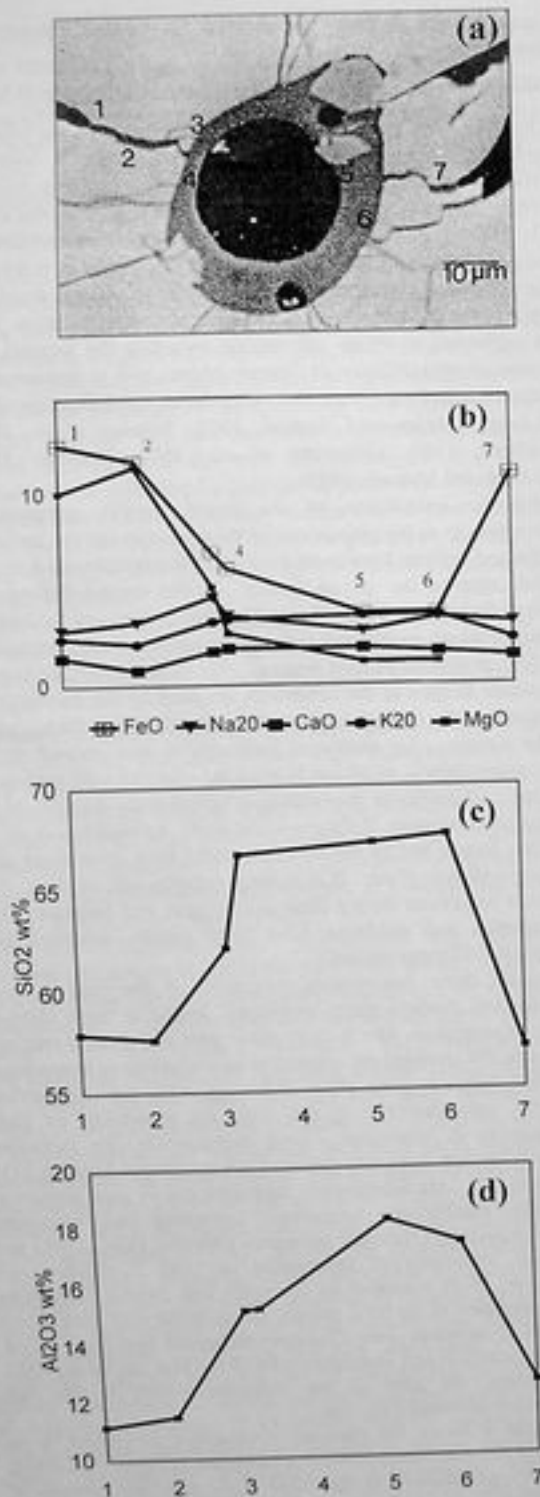
composition of the glass inside the inclusion and close to the inclusion walls remains rich in SiO_2, Al_2O_3, and K_2O, and poor in FeO and MgO (Table 5). This also holds for nondecrepitated glass inclusions.

The similarity of the glass compositions of heated and unheated inclusions indicates that the glass is not a residual glass formed after the inclusion was closed. Thus, our heating experiments (Table 4) strongly support heterogeneous trapping.

Dissolution of the host olivine in the melt and possible diffusion of Fe and Mg from the host into the glass can occur during the heating experiment. This can be detected by elevated contents of both elements and their positive correlation in the glass of heated inclusions (Table 1 and Fig. 4). By dissolving the host mineral, we are adding the olivine component to the liquid and, thus, we can approach the possible composition of the initial liquid trapped at that given temperature and preserved by the quenching of the glass inclusions. Experiments undertaken to up to 900 °C (Table 1) have not dissolved enough host olivine to approach equilibrium. However, in the experiments performed at 1200 °C, the distribution coefficient, $[(Fe/Mg)_{ol}/(Fe/Mg)_{Liq}]$, for olivine and liquid, $K_d =$ 0.317, indicates conditions near to equilibrium. Considering that the olivine–liquid K_d values decrease with increasing alkali content of the coexisting liquid (Baker et al., 1996; Takahashi, 1978; Falloon et al., 1997) and taking into account the experimental data of Takahashi (1978), performed at 1 atm and reducing conditions ($CO_2/H_2 \sim 1$), similar to the conditions for our Chassigny heating experiments, for a total content of alkalis in the liquid of 6.8 wt% (mean value of the content of alkalis in six heated inclusions at 1200 °C, Table 1), the calculated K_d value of 0.317 is in good agreement with equilibrium conditions (Fig. 6).

These results show that heating runs were of long enough duration to achieve dissolution of the host. However, some crystalline phases still remained inside the inclusion. An explanation for this situation is to consider that both the host olivine and some of the included phases may have nucleated above 1200 °C. However, if this is the case, it is difficult to consider these phases as daughter crystals formed under a closed-system cooling after inclusion formation.

The chemical composition of the silica-alkali-rich liquid that has achieved near-equilibrium conditions with the host is clearly different from that previously obtained by Johnson et al. (1991). The similarity in the glass composition before and after heating strongly suggests a stable host–glass relationship and thus heterogeneous trapping.

TABLE 5. Scanning electron microscope analyses of a glass from heated inclusion (1200 °C).*

	1	2	3	4	5	6	7
SiO_2	57.9	58.3	62.2	67.0	68.4	68.1	57.7
TiO_2	0.37	0.00	0.41	0.14	0.04	0.53	0.00
Al_2O_3	11.2	11.6	15.3	15.3	18.5	17.5	12.7
FeO	12.6	11.7	6.9	6.1	3.7	3.7	11.0
MnO	0.74	0.56	0.53	0.34	0.00	0.10	0.17
MgO	10.1	11.5	5.1	2.68	1.17	1.18	11.4
CaO	1.48	0.78	1.73	1.89	1.89	1.68	1.43
Na_2O	2.88	3.2	4.6	3.6	2.8	3.5	3.2
K_2O	2.46	2.14	3.3	3.4	3.6	3.6	2.3
Total	100	100	100	100	100	100	100

Points 1, 2, and 7 = glass inside fracture; points 3 to 6 = glass inside the inclusions. Location of points 1 to 7 as in Fig. 5.
*In wt%.

FIG 5. Backscatter electron scanning image of a heated multiphase inclusion with points indicating SEM analysis. (b–d) Compositional variation of major elements in glass in weight percent.
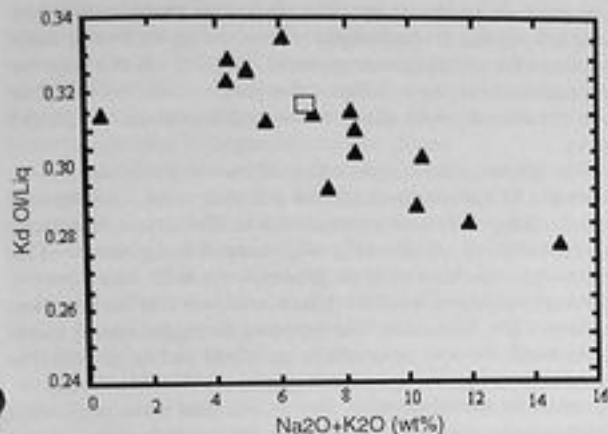
FIG 6. Olivine/liquid K_d (Fe/Mg) vs. total alkali content (weight percent). Plot symbols as follows: ▲ = Takahashi, 1978; □ = Chassigny heated glass-bearing inclusions (1200 °C).

Element Distribution in Glass Inclusions with Depth

Glass in heated inclusions (Fig. 3) has increased orthoclase contents as compared to the unheated glass. Some of these glasses project onto the minimum of the Q–Ab–Or system at 1 bar P_{H_2O} (Johannes and Holtz, 1996).

The variation observed could suggest that the glass is not homogeneous with respect to certain elements (e.g., K_2O, CaO). These inhomogeneities could be the result of a remobilization of some species in a post-entrapment event.

If the alkalis were sampled by the inclusions as solid phases that subsequently were dissolved in the glass in a heating event that created the radial cracks, then some K could have been redeposited in these cracks during this event. Another possibility is that K was added by a metasomatic process. This K then moved into the inclusion during the heating and melting experiment that led to a new homogenized glass composition.

The Rb contents vary between 8 and 210 ppm and are in agreement with those reported by Righter et al. (1997). Strontium, however, has less variable abundances. All inclusions have high contents of Sr (between 560 and 940 ppm), except inclusion 125. The Rb/Sr ratio of the glass of inclusions is nonchondritic, highly variable, and ranges from 0.014 to 0.223. It is positively correlated with the Rb content and approaches the chondritic value (0.295) in the most Rb-rich glass (210 ppm, Table 5). The Rb content is roughly correlated with the K content. The K/Rb ratio is also nonchondritic, with the exception of the two most Rb-rich glasses that have chondritic K/Rb ratios (245 and 234, respectively). We believe that this cannot be a coincidence but rather is an indication for a chondritic rather than a fractionated planetary source of the trapped phases and the fluids associated with them. (Note: we use "fluid" for a low-density, supercritical or gas phase and "liquid" for a high-density mobile phase.)

The fact that primary inclusions hosted by a given olivine have so highly variable Rb/Sr ratios and that are also independent of the inclusion type suggests that

glasses possibly sampled different amounts of Rb and Sr precursor phases. The chemical inhomogeneity of glass in one and the same inclusion also points in this direction.

Alternatively, compositions could have been disturbed by late processes that mobilized these elements. However, mobilization would only have been possible from inclusions that were opened by cracks but not from sealed ones. The degree of variability of the abundances indicates that Rb must have been much more mobile than Sr.

All inclusions have fairly high contents of N, which also appears to be highly inhomogeneously distributed (Table 3). Information concerning the homogeneity of N distribution is obtained by considering both the position of the N peak compared to that of the standard glass and the shape of the nuclear probe spectra (Fig. 7). The shift of the N peak toward lower energy indicates that the information comes from zones located below the glass' surface. Several considerations in the treatment of the data, concerning mainly the incidental and transmitted energy, allow the calculation of the depths from which the information comes (Pyrole program; Trouslard, 1995). As a result, N appears to be concentrated in certain zones of the inclusions with highly variable but increasing abundance with depth. For example, inclusion 125 shows a highly inhomogeneous distribution of N: at the surface, from 0 to 6 μm depth, the N content is 160 ppm; the next zone, from 6 to 14 μm, contains 4780 ppm; and the third one, from 14 to 28 μm, contains 7450 ppm. In only one inclusion (122) does N appear to be homogeneously distributed (540 ppm). This homogeneous distribution (which is similar to that of the standard glass) indicates that the heterogeneities seen in the other glasses cannot be attributed to experimental conditions. The distribution pattern of N seems to be different for each inclusion. Because the concentration is related to a man-made plane, it must be of secondary origin and very likely due to loss of N from the surface, perhaps during analyses. This behavior implies a highly volatile N species, the nature of which is unknown. However, the very different N contents in different glasses point to a heterogeneous acquisition via a solid phase.
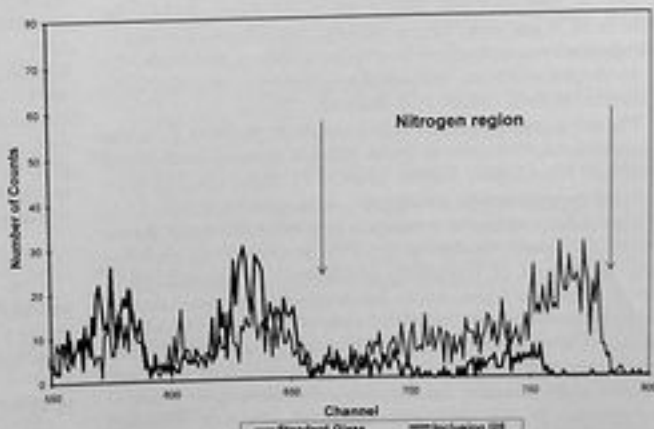

FIG. 7. Comparison of the N spectra of the standard glass and the glass of a Chassigny inclusion. Note the different shape and the shift toward low energy in the glass inclusion spectrum with respect to that of the standard glass.

Possible Mechanism of Formation of Chassigny Inclusions

How to reconcile our results, which suggest that formation of Chassigny inclusions could very likely be the result of heterogeneous trapping of preexisting phases where the SiO_2-rich glass precursor could coexist in equilibrium with the host olivine, with the previously developed homogeneous trapping concept? How to compare a model where a melt is involved with one that, because of the absence of bubbles in all types of inclusions, strongly suggests low sub-igneous temperatures prevailing during entrapment?

In the discussion of the data, we have constantly contrasted our results to igneous processes that have been invoked to explain either the compositional data or the texture of Chassigny inclusions. In doing so, we see that many of these observations do not fit the classical scenario generally proposed for the formation of Chassigny. It is not our intention to ignore the detailed work performed on Chassigny for many years, but our new observations and data suggest a genetic model radically different from the standard SNC meteorite model.

A possible mechanism to consider is that the host olivine and the glass-bearing inclusions could have been formed at subigneous temperatures by aggregation of precipitates from a fluid phase. Thereby the constituents of the inclusions got trapped by the growing olivine. The most abundant "contamination" phase in the fluid must have been the precursor(s) of the glass. They got stuck to the growing olivine's surface and possibly triggered the nucleation of imperfections in the crystal that eventually became glass-bearing inclusions. Many of the such-formed imperfections collected only the glass precursor(s) and apparently were closed too early, before they could collect other phases. They later became the pure glass inclusions which—on average—are clearly smaller than the other inclusions that, in addition, also sampled one or more mineral phases. These subsequently became the monocrystal and multiphase inclusions. This way the heterogeneous phase abundances and phase compositions of the inclusions can be explained. The highly variable alkali contents and, in particular, the variable Rb/Sr and K/Rb ratios of the glass require solid precursors. They could have been amorphous or crystalline and one of them, the one richest in Rb and Sr, had chondritic Rb/Sr and K/Rb ratios. Also, the precursor of N was very likely a solid that was trapped in a highly heterogeneous way in the glass-bearing inclusions in the olivine.

As the precursors were all solid during trapping, a bubble cannot be expected to form, exactly as is observed.

The radial cracks surrounding the inclusions are likely to be due to an overpressure developed by an increase of the volume of the inclusions. This implies that the glass of the inclusions must have increased its volume after entrapment. This situation is difficult to envisage if the precursor of the glass is a melt that will shrink during cooling. A volume increase is, however, possible if the glass had solid (amorphous or crystalline) precursors. A post-entrapment heating event could have led to an overpressure in the inclusions that consequently caused radial cracking of the host. The heating should not have reached, however, the liquidus temperature of the glass, because in that case, the cracks would have been filled with the glass melt, which is not the case. Another way to create an overpressure in the inclusions could be chemical alteration. However, because the well-isolated inclusions are also surrounded by cracks and have heterogeneous glass compositions, this mechanism appears to be unlikely. A heating event clearly is the more likely process because the glass is free of cracks, implying that

it was soft during the event. The absence of cracks in the glass could indicate that the temperature reached during the heating event was above the softening temperature of the glass. In this way, the brittle minerals inside and around the glass cracked but the glass itself did not. It could also not flow and thus could not fill the cracks.

The inhomogeneous distribution of mainly Rb in the glasses could also be a consequence of such a heating event. Because the most Rb-rich glasses have a near-chondritic Rb/Sr ratio, they could be representative of the originally trapped component. The nonchondritic Rb/Sr ratios of the glasses poorer in Rb than those are all subchondritic and could have been established by mobilization and loss of Rb. This could have happened during the heating event during which Rb was preferentially mobilized and in part left the inclusion *via* the freshly opened cracks. This mechanism is supported by the observation that glasses that were artificially heated usually are richer in K than the original glass, which indicates gain of K during the heating event (Table 4), and that K could have come from the cracks where it was deposited during the early heating event that caused the cracking.

The approach of the richest precipitates toward chondritic Rb/Sr ratios indicates a primitive, possibly chondritic reservoir. The SNC meteorites have fairly recently disturbed ages (Jagoutz, 1997a,b; Jagoutz and Dreibus, 1997; Borg *et al.*, 1996). This disturbance could be related to the heating event that produced the glass, the radial cracks in the host olivine, and the mobilization of alkalis from the glasses into the cracks. The possible involvement of a chondritic reservoir in the evolution of Chassigny comes as no surprise, because several primitive features have previously been noted in Chassigny (and other SNC meteorites). In particular, data presented by Jagoutz (1996) suggest a very early (primordial?) Nd depletion and an excess abundance of ^{142}Nd in Chassigny that indicates the presence of live ^{146}Sm (half-life 103 Ma). Birck and Allègre (1994) report chondritic Os-isotopic abundances, and the trapped noble gases in Chassigny have isotope abundances similar to those of the sun (Ott, 1988; Mathew *et al.*, 1998). Several links between SNC meteorites and chondrites have even led to the suggestion that CI chondrites might come from Mars (Brandenburg, 1996). There appears to be growing evidence for the SNC meteorites having some primitive roots, most of it pointing towards sub-igneous temperature events. These indications are all in line with our findings that glass-bearing inclusions in Chassigny olivine are of non-igneous origin and have been trapped at low temperatures. Consequently, the host olivine must have formed at that low temperature in a non-igneous way, very likely by precipitation from a fluid. Also, the inhomogeneous distribution of N in the glasses requires a solid precursor and is incompatible with an igneous origin of the Chassigny olivine and its glass-bearing inclusions.

CONCLUSION

The standard SNC meteorite model has related the glass inclusions in minerals of Chassigny to parent magma trapping during the growth of the host from that melt. However, our results demonstrate that the inclusions in Chassigny olivine are not the product of a post-entrapment closed-system evolution of an originally homogeneous melt.

Detailed petrographic studies of all types of glass-bearing inclusions, the chemical composition of the glass in the different types of inclusions, and their high contents of N, as well as heating experiments, point to an origin by heterogeneous trapping of crystals and solid glass precursors in the Chassigny olivine. In addition, the

compositional variability of glass-bearing inclusions, the lack of a differential shrinkage between the glass precursor and the host, and the absence of cracks in the glass suggest not only that olivines have sampled heterogeneous phases in varying proportions but that this trapping could have happened at fairly low temperatures that prevented chemical homogenization of the glasses.

The nonhomogeneous glass compositions indicate chemically heterogeneous precursors for the glass or mixing of precursor components shortly before or during trapping. This way also opens the possibility for the coexistence of chemically equilibrated host olivines with fresh, nondevitrified glass and nonequilibrated pyroxenes. These new data suggest low temperatures prevailing during the heterogeneous trapping and thus, a likely non-igneous origin for the primary glass-bearing inclusions in Chassigny olivine.

The results of our studies of glass-bearing inclusions in Chassigny olivine have direct implications for the formation of the host and suggest that Chassigny likely was formed at sub-igneous temperatures, probably by aggregation of precipitates from a fluid (gas) phase. There are indications for a primitive, chondrite-like source for that fluid. A late heating event possibly led to a redistribution of volatile species, softening of the glass, and cracking of the crystalline phases, inclusive of the host olivine.

REFERENCES

BAKER M. B., HIRSCHMANN M. M., STOLPER E. M. AND GHIORSO M. S. (1996) Quest for low degree mantle melts. *Nature* **381**, 286.

BIRCK J. L. AND ALLEGRE C. L. (1994) Contrasting Re/Os magmatic fractionation in planetary basalts. *Earth Planet. Sci. Lett.* **124**, 139–148.

BOGARD D. D. AND JOHNSON P. (1983) Martian gases in an Antarctic meteorite. *Science* **221**, 651–654.

BORG L. E., NYQUIST L. E., TAYLOR L. A., WIESMANN H. AND SHIH C-Y. (1996) Rubidium-Strontium age and initial $^{87}Sr/^{86}Sr$ of basaltic shergottite QUE 94201 (abstract). *Meteorit. Planet. Sci.* **31 (Suppl.)**, A18–A19.

BOYNTON W. V., STARZYK M. P. AND SCHMITT R. A. (1976) Chemical evidence for the genesis of the ureilites, the achondrite Chassigny and the nakhlites. *Geochim. Cosmochim. Acta* **40**, 1439–1447.

BRANDENBURG J. E. (1996) Mars as the parent body of the CI carbonaceous chondrites. *Geophys. Res. Lett.* **23**, 961.

BUNCH T. E. AND REID A. M. (1975) The nakhlites, Part I: Petrography and mineral chemistry. *Meteoritics* **10**, 303–315.

CLOCCHIATTI R. (1975) Les inclusions vitreuses des cristaux de quartz: Étude optique, thermometrique et cimique. Applications géologiques. *Mém. Soc. France*, 1–96.

CLOCCHIATTI R. AND MASSARE D. (1985) Experimental crystal growth in glass inclusions: The possibilities and the limits of the method. *Contrib. Mineral. Petrol.* **89**, 193–204.

CLOCCHIATTI R., HAVETTE A., WEISS J. AND WILHELM S. (1978) Les bytownites du rift d'Asal. *Bull. Minéral* **101**, 66–76.

DELANO J. W. AND HANSON B. (1996) Liquid immiscibility: Cause of compositional heterogeneity in tektites (abstract). *Lunar Planet. Sci.* **27**, 305–306.

EL GORESY A., WOPENKA B., CHEN M. AND KURAT G. (1997) The saga of maskelynite in Shergotty (abstract). *Meteorit. Planet. Sci.* **32 (Suppl.)**, A38–A39.

FALLOON T. J., GREEN D. H., O'NEILL H. ST. C. AND HIBBERSON W. O. (1997) Experimental test of low degree peridotites partial melt composition: Implication for the nature of anhydrous near-solidus peridotites melts at 1 GPa. *Earth Planet. Sci. Lett.* **152**, 149–162.

FLORAN R. J., PRINZ M., HLAVA P. F., KEIL K., NEHRU C. E. AND HINTHORNE J. R. (1978) The Chassigny meteorite: A cumulate dunite with hydrous amphibole-bearing melt inclusions. *Geochim. Cosmochim. Acta* **42**, 1213–1229.

HARVEY R. P. AND MCSWEEN H. Y., JR. (1991) Parental magmas of the nakhlites: Clues from the mineralogy of magmatic inclusions (abstract). *Meteoritics* **26**, 343.

HARVEY R. P. AND MCSWEEN H. Y., JR. (1992) Parent magma of the nakhlite meteorites: Clues from melt inclusions. *Earth Planet. Sci. Lett.* **111**, 467–482.

IKEDA Y. (1998) Petrology of magmatic inclusions in the Allan Hills 77005 lherzolitic shergottite. *Meteorit. Planet. Sci.* **33**, 803–812.

JOHANNES W. AND HOLTZ F. (1996) *Petrogenesis and Experimental Petrology of Granitic Rocks*. Springer, Berlin, Germany. 335 pp.

JAGOUTZ E. (1996) Nd isotopic systematics of Chassigny (abstract). *Lunar Planet. Sci.* **27**, 597–598.

JAGOUTZ E. (1997a) Why the SNC meteorites might not come from Mars. In *Conf. Early Mars: Geology and Hydrologic Evolution, Physical and Chemical Environments, and the Implication for Life* (eds. M. S. Clifford, A. H. Treiman, H. Newsom and J. D. Farmer), pp. 42–43. LPI Contrib. No. 916, LPI, Houston, Texas, USA.

JAGOUTZ E. (1997b) Isotopic constraints on differentiation and evolution of SNC meteorites (abstract). *Lunar Planet. Sci.* **28**, 651–652.

JAGOUTZ E. AND DREIBUS G. (1997) On the significance of internal ages and associated chemical changes in SNC meteorites (abstract). *Meteorit. Planet. Sci.* **32 (Suppl.)**, A66–A67.

JOHNSON M. C., RUTHERFORD M. J. AND HESS P. C. (1991) Chassigny petrogenesis: Melt compositions, intensive parameters, and water contents of Martian (?) magmas. *Geochim. Cosmochim. Acta* **55**, 349–366.

KURAT G. (1988) Primitive meteorites: An attempt towards unification. *Phil. Trans. R. Soc. Lond.* **A 325**, 459–482.

LONGHI J. AND PAN V. (1989) The parent magmas of the SNC meteorites. *Proc. Lunar Planet. Sci. Conf.* **19th**, 451–464.

MASON B., NELEN J. A., MUIR P. AND TAYLOR S. R. (1975) The composition of the Chassigny meteorite. *Meteoritics* **11**, 21–27.

MATHEW K. J., KIM J. S. AND MARTI K. (1998) Martian atmospheric components of xenon and nitrogen in the Shergotty, Nakhla, and Chassigny group meteorites. *Meteorit. Planet. Sci.* **33**, 655–664.

MCSWEEN H. Y., JR. (1985) SNC meteorites: Clues to Martian petrologic evolution? *Rev. Geophys.* **23**, 391–416.

MCSWEEN H. Y., JR. (1994) What we have learned about Mars from SNC meteorites. *Meteoritics* **29**, 757–779.

MOSBAH M., BASTOUL A., CUNEY M. AND PIRONON J. (1993) Nuclear microprobe analysis of 14N and its application to the study of ammonium-bearing minerals. *Nucl. Instrum. Method.* **B77**, 450–456.

MYSEN B. O., VIRGO D., POPP R. K. AND BERTKA C. (1998) The rôle of water in Martian magmatic systems. *Am. Mineral.* **83**, 942–946.

NAKAMURA N. (1982) Origin and evolution of the Nakhla meteorite inferred from the Sm-Nd and U-Pb systematics and REE, Ba, Sr, Rb and K abundances. *Geochim. Cosmochim. Acta* **46**, 1555–1573.

OTT U. (1988) Noble gases in SNC meteorites: Shergotty, Nakhla, Chassigny. *Geochim. Cosmochim. Acta* **52**, 1937–1948.

PRINZ M., HLAVA P. H. AND KEIL K. (1974) The Chassigny meteorite: A relatively iron-rich cumulate dunite. *Meteoritics* **9**, 393–394.

ROEDDER E. (1979) Origin and significance of magmatic inclusions. *Bull. Mineral.* **102**, 487–510.

ROEDDER E. (1984) Fluid Inclusions. *Rev. Mineral.* **12**, 644 pp.

RIGHTER K., HERVIG R. L. AND KRING D. A. (1997) Ion microprobe analyses of SNC meteorite melt inclusions (abstract). *Lunar Planet. Sci.* **28**, 1181–1182.

RIGHTER K., HERVIG L. R. AND KRING D. A. (1998) Accretion and core formation on Mars: Molybdenum contents of melt inclusions glasses in three SNC meteorites. *Geochim. Cosmochim. Acta* **62**, 2167–2177.

SCHIANO P., BOURDON B., CLOCCHIATTI R., MASSARE D., VARELA M. E. AND BOTTINGA Y. (1998) Low-degree partial melting trends recorded in upper mantle minerals. *Earth Planet. Sci. Lett.* **160**, 537–550.

SOBOLEV A. V. AND NIKOSIAN I. K. (1994) Petrology of long-lived mantle plume magmatism: Hawaii, Pacific and Reunion Island, Indian Ocean. *Petrology* **2**, 111–144.

SOBOLEV V. S. AND KOSTYUK V. P. (1975) Magmatic crystallization as bases on the study of melt inclusions. Nauka Siberian Branch, Novosibirsk.

SOBOLEV V. S., BAKUMENKO I. T. AND KOSTYUK V. P. (1976) The Possibility for using Melt Inclusions for Petrologic Conclusions. Akad. Nauk. S.S.S.R., Siberian branch Geol. I Geofiz. **5**, 146–149. (In Russian; translated in *Fluid Inclusions Research, Proceedings of COFFI* **9**, 178–181).

STOLPER E. AND MCSWEEN H. Y., JR. (1979) Petrology and origin of the sherogottite meteorites. *Geochim. Cosmochim. Acta* **43**, 1475–1498.

TAKAHASHI E. (1978) Partitioning of Ni^{2+}, Co^{2+}, Fe^{2+}, Mn^{2+} and Mg^{2+} between olivine and silicate melts. Compositional dependence of partition coefficients. *Geochim. Cosmochim. Acta* **42**, 1829–1844.

TREIMAN A. H. (1986) The parental magma of the Nakhla achondrite: Ultrabasic volcanism on the shergottite parent body. *Geochim. Cosmochim. Acta* **50**, 1061–1070.

TREIMAN A. H. (1990) Complex petrogenesis of the Nakhla (SNC) meteorite: Evidence from petrography and mineral chemistry. *Proc. Lunar Planet. Sci. Conf.* **20th**, 273–280.

TREIMAN A. H. (1993) The parent magma of the Nakhla (SNC) meteorite, inferred from magmatic inclusions. *Geochim. Cosmochim. Acta* **57**, 4753–4767.

TROUSLARD P. (1995) PYROLE, Un logiciel au service des analyses par faisceau d'ions. *Rapport* **CEA-R-5703**, 1–30.

WADHWA M. AND CROZAZ G. (1995) Trace and minor elements in minerals of nakhlites and Chassigny: Clues to their petrogenesis. *Geochim. Cosmochim. Acta* **59**, 3629–3645.

WATSON L. L., HUTCHEON I. D., EPSTEIN S. AND STOLPER E. M. (1994) Water on Mars: Clues from deuterium/hydrogen and water contents of hydrous phases in SNC meteorites. *Sciences* **265**, 86–90.

WOOD C. A. AND ASHWAL L. D. (1981) SNC meteorites: Igneous rocks from Mars? *Proc. Lunar Sci. Conf.* **12th**, 1359–1376.

ZAPUNNYY S. A., SOBOLEV A. V., BOGDANOV A. A., SLUTSKIY A. B., DMITRIYEV L. V. AND KUNIN L. L. (1989) An apparatus for high-temperature optical research with controlled oxygen fugacity. *Geochem. Internat.* **26**, 120–128.